Published by IOP Publishing for Sissa Medialab

Received: *September 26, 2019*
Revised: *December 2, 2019*
Accepted: *January 14, 2020*
Published: *February 14, 2020*

21st International Workshop on Radiation Imaging Detectors
7–12 July 2019
Crete, Greece

Improvement of a spectrum-to-dose conversion function for electronic personal dosimeters

K. Park,[a] J. Kim,[a] K.T. Lim,[a] G. Kim,[a] M. Lee,[a] H. Kim[b] and G. Cho[a,1]

[a] *Department of Nuclear and Quantum Engineering, Korea Advanced Institute of Science and Technology, 291 Daehak-ro, Yuseong-gu, Daejeon, 34141, Republic of Korea*
[b] *IRIS Co., Ltd., 193, Munji-ro, Yuseong-gu, Daejeon, 34051, Republic of Korea*

E-mail: gscho@kaist.ac.kr

Abstract: For electronic personal dosimeters (EPDs) based on a spectroscopy system, it is necessary to accurately measure the dose in real-time from the gamma energy spectra. The method of spectrum-to-dose conversion is being used instead of the method of count-to-dose conversion. The $G(E)$ function, a typical method of spectrum-to-dose conversion has been applied to various instruments due to its good dose measurement performance and the advantage of real-time measurements. In this manuscript, we present a method to increase the accuracy of $G(E)$ function for the EPD consisting of a 3×3 mm^2 PIN diode coupled with a $3 \times 3 \times 3$ mm^3 CsI(Tl) scintillator. The new $G(E)$ function was calculated using the adaptive moment estimation (ADAM) method based on Monte Carlo simulation. The proposed $G(E)$ function is verified by comparison with the least-square method (LSM), which is the conventional method for calculating the $G(E)$ function and with the gradient-descent method (GDM), which is the basis for the ADAM. The relative difference was acquired to compare the converted dose value using each $G(E)$ function by using ^{241}Am, ^{57}Co, ^{22}Na, ^{137}Cs, ^{54}Mn and ^{60}Co radioisotopes. In addition, the energy response to ^{137}Cs of each $G(E)$ function was obtained. The relative difference of $G(E)$ function according to LSM, GDM, and ADAM was in the range of ±28.54, ±12.59, and ±9.9%, respectively, and the energy response to ^{137}Cs was 0.71 to 1, 0.87 to 1.02, and 0.9 to 1.03, respectively.

Keywords: Dosimetry concepts and apparatus; Analysis and statistical methods; Data processing methods; Models and simulations

[1]Corresponding author.

https://doi.org/10.1088/1748-0221/15/02/C02018

Contents

2020 JINST 15 C02018

1 Introduction

In the field of dosimetry, radiation monitoring of a specific area is required to measure the energy of the radiation deposited on the human body and to evaluate the risk of health effects. The International Commission on Radiological Units and Measurements (ICRU) has defined measureable quantities that provide convenient and appropriate evaluations of the equivalent and effective dose for radiation [1]. The International Commission on Radiological Protection (ICRP) recommends that the appropriate dose for monitoring the effective dose through environmental monitoring is the ambient dose equivalent $H^*(10)$ [2]. In fact, the ICRU defines $H^*(10)$ as 'the ambient dose equivalent, $H^*(10)$, at a point in a radiation field is the dose equivalent that would be produced by the corresponding expanded and aligned field at a depth of 10 mm in the ICRU sphere, on the radius opposing the direction of the aligned field' [1].

The vast majority of detectors used for measuring the $H^*(10)$ are gas-filled detectors, such as a Geiger-Muller (GM) counter or an ionization chamber. In particular, the most popular radiation detectors used dosimeters are GM counters because of their low price. GM counters provide only counts or count rates, so the count-to-dose conversion factor is used to obtain the dose value. Despite the use of an energy-compensated filter in the detector, the energy response of a GM counter is not independent from energy in the low energy region. In addition, a GM counter cannot provide spectral data, so it is difficult to use for the qualitative and quantitative analysis of radioisotopes. Energy spectra data can be used to acquire the dose and for the qualitative and quantitative analysis of radioisotopes. The ideal scintillator for $H^*(10)$ conversion from the gamma spectra is the plastic scintillator, which is close to tissue equivalent. The light yield of a plastic scintillator is proportional to $H^*(10)$, however, a plastic scintillator must be large for low dose rates due to low efficiency [3]. Furthermore, it is difficult to intuitively identify the types of radioisotopes from the gamma spectra since there is no photo-peak for gamma rays. Therefore, many studies have shown that the $H^*(10)$ from the gamma spectra can be obtained using inorganic scintillators such as NaI(Tl), CsI(Tl) and $LaBr_3$(Ce) [3–6].

There are two common methods for the estimation of $H^*(10)$ from the gamma spectra that have been published. They are called the unfolding method and the $G(E)$ function method. The unfolding method is to determine the fluence of photons from the gamma spectra. The fluence can be acquired by an algorithm, such as the stripping method and the Gravel algorithm using the detector response function [6, 7]. Finally, $H^*(10)$ can be calculated via the fluence-to-$H^*(10)$ conversion factor provided by the ICRP74 publication [8]. It can provide not only the accurate $H^*(10)$ but also identification of the radioisotopes. However, since the calculation takes a long time, and the obtained spectrum is used, it is difficult to check the $H^*(10)$ in real-time, which limits the application of real-time dosimeters. As for the $G(E)$ function method, $H^*(10)$ can be accurately acquired in real time because it provides a conversion factor for each energy in the gamma spectra. The $G(E)$ function can be described by the polynomial function for the power of the natural logarithm and calculated by the least-squares method (LSM) when $H^*(10)$ of the radiation field is known [9–11]. Therefore, the $G(E)$ function method has been utilized in many kinds of dosimeters because it does not require many computational steps for the calculation, and it provides $H^*(10)$ in real-time.

In a previous study, we proposed a small electronic personal dosimeter (EPD) based on a $3 \times 3\,\mathrm{mm}^2$ PIN diode coupled with a $3 \times 3 \times 3\,\mathrm{mm}^3$ CsI(Tl) scintillator that can be used in the range of 40 keV to 2 MeV [12]. In addition, the $G(E)$ function as a dose conversion method was newly acquired using the gradient-descent method (GDM) instead of LSM to satisfy the error rate within 20% in the target energy range. It was confirmed that the error is smaller than that of the conventional LSM-based $G(E)$ function. However, since the GDM uses a fixed learning rate, there is a problem that a non-optimal value or a local minima problem may occur before the optimal value is reached. In this study, the $G(E)$ function was newly calculated by using the adaptive moment estimation (ADAM) method, which can be calculated by adjusting the learning rate that is widely used in machine learning. The gamma spectra data and $H^*(10)$ data that correspond to 5000 discrete energies from 40 keV to 2000 keV with the random number of particle histories randomly were acquired by Monte Carlo simulation using the Monte Carlo N-particle transport code 6 (MCNP6) [13]. The newly acquired ADAM-based $G(E)$ function was applied to the previously designed EPD and verified by converting spectra to $H^*(10)$ using radioisotopes. In addition, we compared the ADAM-based $G(E)$ with the conventional LSM-based $G(E)$ and the GDM-based $G(E)$ of the previous study with error and the energy response.

2 Materials and method

2.1 The method of the $G(E)$

The relationship between the measured spectrum $M(E)$ obtained by the designed EPD and the fluence of the gamma-ray $\phi(E_0)$, where E_0 is the incident gamma-ray energy, can be expressed as

$$M(E) = \int_{E_{\min}}^{E_{\max}} R(E, E_0)\, \phi(E_0)\, dE_0 \tag{2.1}$$

where $R(E, E_0)$ is the response function of the designed EPD which represents the gamma rays of energy E_0 that deposits an energy E into the CsI(Tl) scintillator; $E_{\max}$ is the maximum detectable energy, which is the practical limit of gamma-ray energy; and $E_{\min}$ is the minimum detectable

2020 JINST 15 C02018

energy, which is the noise level of the EPD. In the case of the designed EPD, $E_{\min}$ is 40 keV, and $E_{\max}$ is 2 MeV.

The ambient dose equivalent $H^*(10)(E_0)$ (in μSv/h) generated at a given fluence $\phi(E_0)$ using the fluence-to-ambient dose equivalent conversion coefficient ($H^*(10)(E_0)/\phi(E_0)$), which is equal to

$$\frac{H^*(10)(E_0)}{\phi(E_0)} = \int_{E_{\min}}^{E_{\max}} R(E, E_0)\, G(E)\, dE \tag{2.2}$$

where $G(E)$ is the spectrum-to-dose conversion function. The ambient dose equivalent $H^*(10)$ in multi-energy radiation exposure can be expressed by combining eq. (2.1) and eq. (2.2):

$$\begin{aligned} H^*(10) &= \sum_i \phi(E_i)\,[H^*(10)(E_i)/\phi(E_i)] \\ &= \sum_i \int_{E_{\min}}^{E_{\max}} \phi(E_i)\, R(E, E_i)\, G(E)\, dE \\ &= \int_{E_{\min}}^{E_{\max}} \sum_i \phi(E_i)\, R(E, E_i)\, G(E)\, dE \\ &= \int_{E_{\min}}^{E_{\max}} M(E)\, G(E)\, dE \\ &= \sum_{i=1}^{N} M(E_i)\, G(E_i) \end{aligned} \tag{2.3}$$

where N is the number of channels of the 10-bit analog-to-digital converter (ADC) in the EPD system, which corresponds to 1024 in this case.

According to previous papers using the $G(E)$ function [9–11], $G(E)$ is expressed as eq. (2.4), which is the polynomial function for $\log E$:

$$G(E) = \sum_{K=1}^{K_{\max}} A(K)\,(\log E)^{K-M-1} \tag{2.4}$$

where $A(K)$ is a parameter, M is a constant, and $K_{\max}$ is the number of $A(K)$ terms.

Several previous studies have calculated parameter $A(K)$ in the $G(E)$ by applying the LSM. In addition, in our previous study, $A(K)$ was obtained using the GDM to improve the accuracy of dose conversion. In the case of the LSM, it is very sensitive to the presence of unexpected data points in the data set that could be resulting from different external factors such as the malfunction of the detector system, the inherent statistical fluctuation arising from the surrounding environment, and the usage of inappropriate input data. As a result, one or two irregularities in the input data can distort the results of the output data from the LSM significantly. The GDM, on the other hand, can find an optimal value over LSM in terms of searching an optimal estimate through an iterative process. However, in the GDM, the results are different concerning hyperparameters, such as the learning rate and the number of iterations. In addition, non-optimal results can be derived before the optimal value is reached or a local minima problem can occur because a fixed learning rate is used [14].

2020 JINST 15 C02018

2.2 Adaptive moment estimation (ADAM) based $G(E)$ function

A GDM-based parameter optimization method has been developed to overcome the above-mentioned disadvantages of GDM [14]. The ADAM method is one of the methods to optimize the parameters by changing the learning rate for each variable [15]. The advantage of the ADAM is that the learning rate is not affected by the rescaling of the gradient, so it can be reliably optimized using any function. In addition, the learning rate can be adapted by reference to the gradient of the past. Due to these advantages, ADAM is currently used for research on artificial neural networks. Before application of the ADAM to the $G(E)$ function, it is necessary to obtain the spectral data and the corresponding $H^*(10)$ data within the measured energy range. Therefore, a dataset of 5,000 spectra was obtained by randomly generating mono-energy ranging from 40 keV to 2 MeV and the number of particle histories between 10^3 and 10^6 via Monte-Carlo simulation using MCNP6 to accurately fit the $G(E)$ function because there are not enough radioisotope sources available to cover the energy region. Furthermore, it is necessary to include information on the uncertainty, such as a low-count spectrum. To apply the ADAM to the $G(E)$ function, it can be calculated using the mean-square error (MSE) in the same way as the GDM. The MSE function for the ADAM can be expressed as

$$\mathrm{MSE}\left[A\left(0\right), A\left(1\right), \ldots, A\left(\mathrm{KMAX}\right)\right] = \frac{1}{J}\sum_{j=1}^{J}\left(H^*\left(10\right)_{\mathrm{exp},m} - H^*\left(10\right)_{\mathrm{known},m}\right)^2 \tag{2.5}$$

where $H^*(10)_{\mathrm{exp}}$ is the expected ambient dose equivalent, $H^*(10)_{\mathrm{known}}$ is the known ambient dose equivalent calculated from the Monte-Carlo simulation, and J is the number of simulated spectra, which is equal to 5,000.

The first moment estimate (the mean, m_t) and second raw moment estimate (the uncentered variance, v_t) used in ADAM for the $G(E)$ function can be expressed as

$$m_t = \beta_1 m_{t-1} + (1-\beta_1)\left(\frac{\partial}{\partial A\left(K\right)}\mathrm{MSE}\left[A\left(0\right),\ A\left(1\right), \ldots, A\left(K_{\max}\right)\right]\right) \tag{2.6}$$

$$v_t = \beta_2 v_{t-1} + (1-\beta_2)\left(\frac{\partial}{\partial A(K)}\mathrm{MSE}[A\left(0\right), A\left(1\right), \ldots, A\left(K_{\max}\right)]\right)^2 \tag{2.7}$$

where β_1 is 0.9, β_2 is 0.999, and moment estimates (m_t and v_t) are initialized to zero and are biased towards zero during the initial time steps when the decay rates are small. To counteract these biases, a corrected bias calculation of the first and second moment estimates is necessary. The corrected moment estimates are expressed as

$$\hat{m}_t = \frac{m_t}{1-\beta_1^t} \tag{2.8}$$

$$\hat{v}_t = \frac{v_t}{1-\beta_2^t} \tag{2.9}$$

The parameter $A(K)$ in the $G(E)$ function can be obtained via the ADAM update rule as shown in eq. (2.10) by using the corrected moment estimates for $A(K)$:

$$A\left(K_{i+1}\right) = A\left(K_i\right) - \frac{\alpha}{\sqrt{\hat{v}_t} + \epsilon}\hat{m}_t \tag{2.10}$$

where i is the number of iterations, α is the learning rate, or in this case, $\alpha = 0.001$, and ϵ is a small value of 10^{-8} to prevent the denominator from becoming zero. The parameter $A(K)$ in the $G(E)$ can be obtained by updating $\hat{m}_t$ and $\hat{v}_t$ through iteration.

2020 JINST 15 C02018

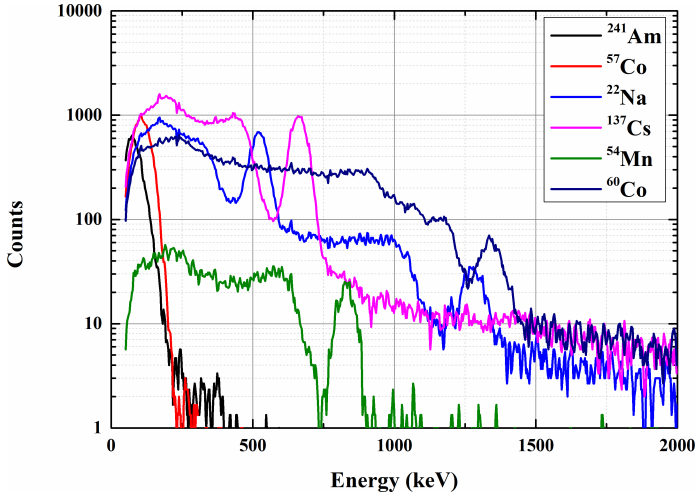

Figure 1. The gamma energy spectra obtained from the designed EPD on radioisotopes.

3 Results and discussion

The gamma energy spectra for radioisotope sources of ^{241}Am, ^{57}Co, ^{22}Na, ^{137}Cs, ^{54}Mn, and ^{60}Co were obtained from the designed EPD, as shown in figure 1. The acquisition time of the spectra was 300 seconds and the distance between the source and the detector was set to 5 cm. In this case, the sensitivity of EPD for $H^*(10)$ for ^{241}Am, ^{57}Co, ^{22}Na, ^{137}Cs, ^{54}Mn, and ^{60}Co were measured as 20.96, 28.34, 0.62, 0.55, 0.46, and 0.28 (cps/μSv/h), respectively. The results show that the energy response to ^{137}Cs is not constant. This is because the discrepancy between the CsI(Tl) scintillator and human tissue is significant in terms of the energy response. Therefore, it is important to acquire an appropriate $G(E)$ function to solve this problem.

The conventional methods of LSM-based $G(E)$ and GDM-based $G(E)$ were additionally conducted compare the proposed ADAM-based $G(E)$ with other methods. In all cases, the constant M in the $G(E)$ function was set to zero because the effect of M on the dose accuracy is negligible [11]. In addition, the parameter $A(K)$ in the $G(E)$ function was calculated for $K_{\max}$ ranging from 2 to 20. The gamma energy spectra in figure 1 were converted to $H^*(10)$ by using each $G(E)$ function. Then, the root-mean-square error (RMSE) and the mean-absolute-percentage error (MAPE) for various $K_{\max}$ values were used to determine the optimal $K_{\max}$ value. In the case of LSM-based $G(E)$, the calculation was performed in the same way as in previous studies. Thus, a total of 99 discrete energies from 40 keV to 2 MeV with a step of 20 keV by MCNP6 were used for calculation. Then, parameter $A(K)$ was obtained through LSM. In the case of GDM-based $G(E)$ and ADAM-based $G(E)$, on the other hand, parameter $A(K)$ was initially set to zero, and the learning rate was set as 0.001. In addition, 5,000 discrete energies that randomly generated energy and the number of particle histories from 40 keV to 2 MeV with various conditions by MCNP6 were used to improve the fitting of the $G(E)$ function. The value of $K_{\max}$ for each method was chosen as $K_{\max} = 17$ for GDM and $K_{\max} = 18$ for ADAM. Figure 2 shows each obtained $G(E)$ function. It can be confirmed that there is a difference between LSM and the other two methods in the low-energy region. In addition, GDM and ADAM show slight differences in the low-energy and high-energy regions.

2020 JINST 15 C02018

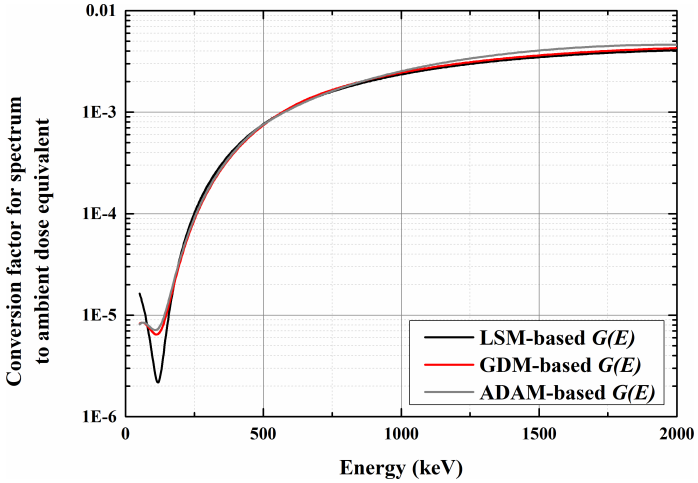

Figure 2. $G(E)$ function with LSM, GDM and ADAM.

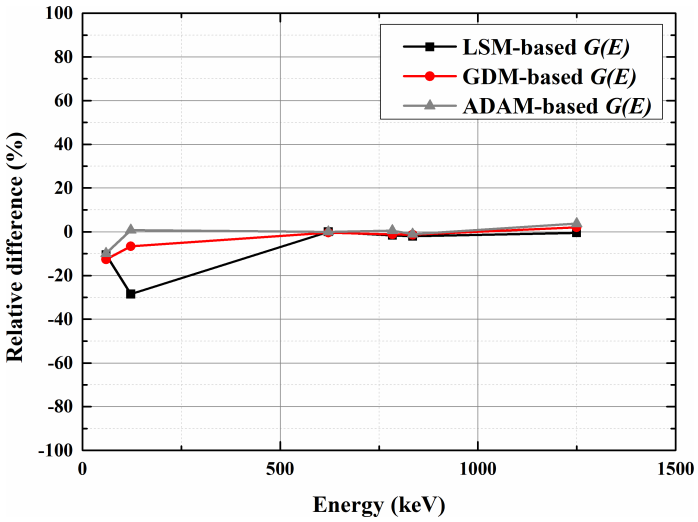

Figure 3. Relative difference for radioisotopes between the $H^*(10)$ converted by the $G(E)$ function and the calculated $H^*(10)$.

Figure 3 shows the relative difference for radioisotopes between the converted $H^*(10)$ by the $G(E)$ function and the calculated $H^*(10)$. The relative differences in $H^*(10)$ for the LSM-, GDM-, and ADAM-based $G(E)$ were in the range of 28.54, 12.59, and 9.9%, respectively. It was found that the large relative difference in the low-energy region for the conventional LSM can be reduced with large amounts of data under various conditions using GDM and ADAM. Furthermore, it was confirmed that the accuracy of the dose can be increased by the ADAM.

The $H^*(10)$ can be finally obtained by multiplying the energy spectra in the EPD by the $G(E)$ function for each energy. Figure 4 shows the gamma spectra of ^{137}Cs and ^{60}Co converted to $H^*(10)$ using ADAM-based $G(E)$. As seen in figure 4, the converted $H^*(10)$ spectrum for ^{60}Co exhibits photo-peaks that are more easily identified than the energy spectra. Therefore, it is advantageous to use the $G(E)$ function for identifying radioisotopes as well as for measuring the $H^*(10)$. In fact, the

2020 JINST 15 C02018

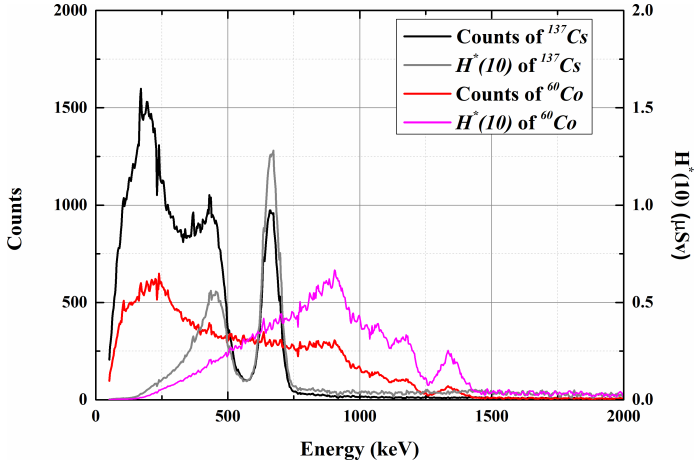

Figure 4. Measured spectra for ^{137}Cs and ^{60}Co and the converted $H^*(10)$ spectra for each radioisotope.

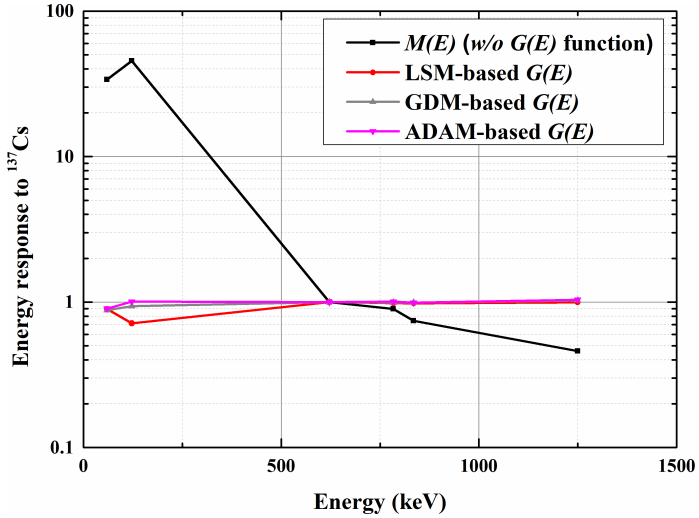

Figure 5. Energy response to ^{137}Cs of $H^*(10)$ for each method.

$H^*(10)$ is the sum of the $H^*(10)$ values for all energies in the converted $H^*(10)$ spectra. It means that the final $H^*(10)$ is acquired by counting the converted $H^*(10)$ spectra. The energy response to ^{137}Cs obtained by counting the converted $H^*(10)$ spectra for each method is shown in figure 5. It was confirmed that the energy response is improved over the original counting method when the $G(E)$ function is used. In addition, the energy responses resulting from LSM, GDM, and ADAM lie in the ranges of 0.71 to 1, 0.87 to 1.02, and 0.9 to 1.03, respectively. Thus, this clearly demonstrates that the ADAM-based $G(E)$ can increase not only the accuracy of the $H^*(10)$ but also the energy response.

4 Conclusion

In this manuscript, the spectrum-to-dose conversion function $G(E)$ was obtained by the ADAM for applying the designed EPD. In addition, we compared the newly obtained $G(E)$ function with

the $G(E)$ obtained by the LSM, which is the conventional method, and $G(E)$ obtained by the GDM, which was used in a previous study using the gamma spectra for ^{241}Am, ^{57}Co, ^{22}Na, ^{137}Cs, ^{54}Mn, and ^{60}Co by the designed EPD. From the results, we demonstrated that the $H^*(10)$ relative differences of all six isotope for LSM, GDM, and ADAM were in the ranges of ±28.54, ±12.59, and ±9.9 %, respectively. In addition, the energy responses to ^{137}Cs for LSM, GDM, and ADAM lie in the ranges of 0.71 to 1, 0.87 to 1.02, and 0.9 to 1.03, respectively for photon energies ranging from 59.5 to 1250 keV. Thus, it can be confirmed that the new ADAM-based $G(E)$ function can increase the energy response as well as the accuracy of the $H^*(10)$. Furthermore, the partial absorption, such as Compton scattering can be reduced, and the photo-peaks can be more intuitively distinguished using the converted $H^*(10)$ spectra by the $G(E)$ function. It is expected that the converted $H^*(10)$ spectra will be advantageous for the identification of various radioisotopes.

Acknowledgments

This work was supported by the Center for Integrated Smart Sensors funded by the Ministry of Science and ICT as Global Frontier Project (CISS-2016M3A6A6929965) and the Nuclear Research & Development Program of the National Research Foundation of Korea (NRF) grant funded by the Ministry of Science, ICT and Future Planning (MISP) (NRF-2018M2A8A5023361).

References

[1] International Commission on Radiation Units and measurements, *Quantities and units in radiation protection dosimetry*, ICRU report 51 (1996).

[2] International Commission on Radiological Protection, *The 2007 recommendations of the International Commission on Radiological Protection*, ICRP Publication 103 (2007).

[3] P. Buzhan, A. Karakash and Y. Teverovskiy, *Silicon photomultiplier and CsI(Tl) scintillator in application to portable $H^*(10)$ dosimeter*, *Nucl. Instrum. Meth.* **A 912** (2018) 245.

[4] R. Casanovas, E. Prieto and M. Salvado, *Calculation of the ambient dose equivalent $H^*(10)$ from gamma-ray spectra obtained with scintillation detectors*, *Appl. Radiat. Isot.* **118** (2016) 154.

[5] C.Y. Yi et al., *Measurement of ambient dose equivalent using a NaI(Tl) scintillation detector*, *Rad. Prot. Dosim.* **74** (1997) 273.

[6] A. Camp and A. Vargas, *Ambient dose estimation $H^*(10)$ from $LaBr_3(Ce)$ spectra*, *Rad. Prot. Dosim.* **160** (2014) 264.

[7] W. Yudong, et al., *Comparison of two spectrum-dose conversion methods based on NaI(Tl) scintillation detectors*, 2018 *JINST* **13** T06004.

[8] International Commission on Radiological Protection, *Conversion coefficients for use in radiological protection against external radiation*, ICRP Publication 74 (1996).

[9] S. Moriuchi and I. Miyanaga, *A spectrometric method for measurement of low-level gamma exposure dose*, *Health Phys.* **12** (1966) 541.

[10] P. Huang, *Measurement of air kerma rate and ambient dose equivalent rate using the $G(E)$ function with hemispherical CdZnTe detector*, *Nucl. Sci. Technol.* **29** (2018) 35.

[11] H. Terada et al., *Spectrum-to-exposure rate conversion function of a Ge(Li) in-situ environmental gamma-ray spectrometer*, *IEEE Trans. Nucl. Sci.* **24** (1977) 647.

2020 JINST 15 C02018

[12] K. Park et al., *Ambient dose equivalent measurement with a CsI(Tl) based electronic personal dosimeter*, *Nucl. Eng. Technol.* **51** (2019) 1991.

[13] Goorley, J.T., et al., *MCNP6 User's Manual, Version 1.0*, Los Alamos Scientific Laboratories, U.S.A. (2013).

[14] S. Ruder, *An overview of gradient descent optimization algorithms*, arXiv:1609.04747.

[15] D.P. Kingma and J. Ba, *Adam: a method for stochastic optimization*, arXiv:1412.6980.

2020 JINST 15 C02018